OXFORD

Neurotensin expression, regulation, and function during the ovulatory period in the mouse ovary[†]

Ketan Shrestha[1], Linah Al-Alem[1], Priscilla Garcia[1], Michelle A. A. Wynn[1], Patrick R. Hannon[1],
Misung Jo[1], Jenny Drnevich[2], Diane M. Duffy[3] and Thomas E. Curry Jr[1,*]

[1]Department of Obstetrics & Gynecology, College of Medicine, University of Kentucky, Lexington, Kentucky, USA
[2]Roy J Carver Biotechnology Center, University of Illinois at Urbana-Champaign, Urbana, Illinois, USA
[3]Department of Physiological Sciences, Eastern Virginia Medical School, Norfolk, Virginia, USA
*Correspondence: Department of Obstetrics and Gynecology, Chandler Medical Center, University of Kentucky, 800 Rose Street, Room MS 331, Lexington, KY
40536-0298, USA. E-mail: tecurry@uky.edu

Abstract

The luteinizing hormone (LH) surge induces paracrine mediators within the ovarian follicle that promote ovulation. The present study explores neurotensin (NTS), a neuropeptide, as a potential ovulatory mediator in the mouse ovary. Ovaries and granulosa cells (GCs) were collected from immature 23-day-old pregnant mare serum gonadotropin primed mice before (0 h) and after administration of human chorionic gonadotropin (hCG; an LH analog) across the periovulatory period (4, 8, 12, and 24 h). In response to hCG, *Nts* expression rapidly increased 250-fold at 4 h, remained elevated until 8 h, and decreased until 24 h. Expression of Nts receptors for *Ntsr1* remained unchanged across the periovulatory period, *Ntsr2* was undetectable, whereas *Sort1* expression (also called *Ntsr3*) gradually decreased in both the ovary and GCs after hCG administration. To better understand *Nts* regulation, inhibitors of the LH/CG signaling pathways were utilized. Our data revealed that hCG regulated *Nts* expression through the protein kinase A (PKA) and p38 mitogen-activated protein kinase (p38MAPK) signaling pathways. Additionally, epidermal-like-growth factor (EGF) receptor signaling also mediated *Nts* induction in GCs. To elucidate the role of NTS in the ovulatory process, we used a *Nts* silencing approach (si-Nts) followed by RNA-sequencing (RNA-seq). RNA-seq analysis of GCs collected after hCG with or without si-Nts identified and qPCR confirmed *Ell2*, *Rsad2*, *Vps37a,* and *Smtnl2* as genes downstream of *Nts*. In summary, these findings demonstrate that hCG induces *Nts* and that *Nts* expression is mediated by PKA, p38MAPK, and EGF receptor signaling pathways. Additionally, NTS regulates several novel genes that could potentially impact the ovulatory process.

Summary Sentence

Nts expression increased 250-fold 4 h after hCG in mouse ovaries and is regulated through classical hCG signaling pathways. Using siRNA followed by RNAseq, *Ell2*, *Rsad2*, *Vps37a*, and *Smtnl2* were identified as NTS downstream targets in granulosa cells.

Graphical Abstract
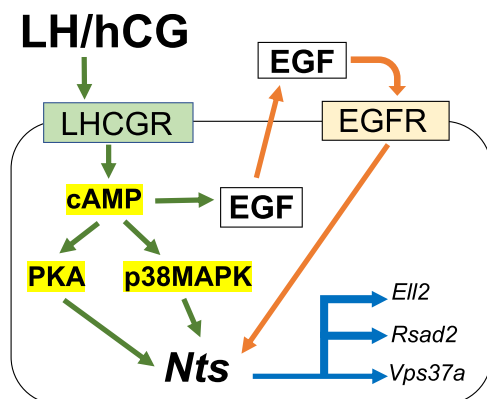
Keywords: neurotensin, ovulation, granulosa cells, siRNA, silencing, RNAseq

Introduction

The midcycle surge of luteinizing hormone (LH) triggers the ovulatory cascade of events within the ovarian follicle leading to oocyte expulsion followed by the formation of the corpus luteum. This initiation of the ovulatory process by the LH surge is accomplished by the production and regulation of paracrine mediators from the follicular cells that express LH receptors [1]. Our recent studies have revealed neurotensin (NTS) as one of the essential paracrine mediators in the ovulatory follicle [2, 3].

NTS is a small 13-amino-acid neuropeptide that was first characterized as a neurotransmitter in neuronal cells. However, NTS has been found throughout the body, such as in the cardiovascular system, the gastrointestinal tract, the endocrine system, and the reproductive system [4–6]. In the ovary, studies have reported that the ovulatory LH surge increases NTS expression in granulosa cells of humans, non-human primates, rats, and cows [2, 3, 7–9]. A recent study in non-human primates has revealed that injecting a NTS-neutralizing antibody into preovulatory macaque follicles yielded ovaries containing entrapped oocytes within unruptured, hemorrhagic follicles [3] demonstrating a key role for NTS in ovulation. However, the potential mechanisms of NTS action in the ovulatory process are unknown.

NTS carries out its function via its three well-characterized receptors: NTSR1, NTSR2, and SORT1 (also known as sortillin or NTSR3). NTSR1 and NTSR2 belong to the family of classical G protein-coupled, seven transmembrane spanning domain receptors whereas SORT1 is a single transmembrane receptor, non-coupled to G-proteins, which belongs to the Vps10p containing domain receptor family [10, 11]. Depending upon the target cells, NTS action is dependent on the specific receptor to which it binds, the abundance of each receptor, the specific tissue location of the NTS receptor, and the interaction between the NTS receptors [12–14]. NTS has been reported to promote cell migration [13, 15], extracellular matrix remodeling [16], and cell cycle/apoptosis [17, 18], all of which are also key cell functions during ovulation and transformation of the follicle into the corpus luteum [19].

Although there is a body of literature on NTS, little is known about the specific actions of NTS in the ovulatory process. Particularly, the role of NTS as a paracrine mediator has not been explored in the periovulatory follicular cells. In the present study, we utilized pregnant mare serum gonadotropin (PMSG)/human chorionic gonadotropin (hCG)-primed immature mouse models to first characterize the expression of NTS and its receptors in the ovary and then investigate the function of NTS during the ovulatory process using an RNA-silencing (RNA-seq) approach, followed by RNA-seq.

Materials and methods

Media and reagents

Unless otherwise specified, all chemicals and reagents were purchased from Sigma-Aldrich Chemical Co. (St. Louis, MO). Culture media and TaqMan Gene Expression Master Mix were purchased from Invitrogen Life Technologies (Carlsbad, CA).

In vivo mouse ovary collection

All animal procedures for these experiments were approved by the University of Kentucky IACUC. Immature female C57BL/6 mice (Charles River Laboratories, Wilmington, MA) at postnatal day (PND) 23–24 were subcutaneously injected with PMSG (5 IU) to stimulate the development of multiple follicles. After 48 h, some animals were euthanized to serve as the control group (0 h). The remaining mice were subcutaneously injected with hCG (2.5 IU) to induce the ovulatory cascade. These animals were euthanized at set times across the periovulatory period (4, 8, 12, and 24 h post-hCG administration). Mice ovulate shortly following the 12 h time point. Whole intact ovaries were collected at the designated time points and stored at –80 °C for later analysis or punctured to collect granulosa cells [20].

Mouse granulosa cell culture

Immature 23–24 PND mice were subcutaneously injected with PMSG (5 IU) as described previously. After 48 h, the animals were euthanized and ovaries were isolated. Briefly, granulosa cells were isolated by follicular puncture, pooled, filtered, pelleted by centrifugation, and resuspended in Opti-MEM medium supplemented with 0.05 mg/mL of gentamycin and 1x ITS (insulin, transferrin, and selenium) as routinely performed in our laboratory [20]. Cells were plated in 12-well dish (250,000 cells/well) and then treated immediately with or without hCG (1 IU/mL), cultured at 37 °C in a humidified atmosphere of 5% CO_2 and collected at the time of culture or after 4, 8, 12, or 24 h of treatment.

To determine the pathways regulating NTS expression, the cells were pre-treated with the inhibitors of the following LH-activated signaling pathways for 1 h: H89 (PKA inhibitor, 10 μM), GF (GF109203x; PKC inhibitor 1 μM), LY (LY294002; PI3K inhibitor 25 μM), PD (PD98059; MEK1/2 inhibitor, 20 μM) or SB (SB203580; p38 MAPK inhibitor 20 μM). Cells were then treated with or without hCG for 4 h in the absence or presence of above-mentioned inhibitors. In parallel, inhibitors of LH-induced paracrine factors were also pre-incubated for 1 h: the EGF receptor inhibitor (AG1478;1 μM), progesterone receptor antagonist (RU486; 1 μM), prostaglandin synthase 2 inhibitor (NS398; 1 μM). These doses have previously been shown to be effective inhibitors of their respective targets [2, 21]. Then, cells were treated with or without hCG in the absence or presence of the above-mentioned inhibitors for 4 h. At the end of culture, cells were collected and mRNA was isolated as described below.

Nts silencing by small interfering RNA

Mouse granulosa cells were isolated from ovaries of PMSG-primed mice. Cells (180,000 cells/well in a 12-well dish) were seeded and transfected immediately before cells could adhere to the wells using Lipofectamine RNAiMAX transfection reagent (Invitrogen, Carlsbad, CA) according to the manufacturer's protocol. Cells were transfected in suspension with 5 nmol/L of a small interfering RNA construct targeting *Nts* (si-Nts; assay s84990; Thermo Fisher Scientific), or with scrambled siRNA (the negative control; si-NC, assay 4390844; Thermo Fisher Scientific). Transfected cells were incubated for 3 h before stimulating with hCG (1 IU/mL), cultured for additional 4 and 12 h, and then harvested.

RNA isolation and sequencing

Total RNA was extracted from granulosa cells transfected with or without si-Nts at 4 and 12 h after hCG using RNeasy Mini Kit (Qiagen, Valencia, CA) with DNase (Qiagen) as per

the manufacturer's instructions as routinely performed in our laboratory [21]. The quality of total RNA was assessed by Bioanalyzer RNA Nano chip kit (Agilent, Santa Clara, CA). RNA-seq and analysis were performed at the Roy J. Carver Biotechnology Center, University of Illinois. The RNAseq libraries were prepared with Illumina's "TruSeq Stranded mRNAseq Sample Prep kit" (Illumina). The libraries were pooled, quantitated by qPCR, and sequenced on two SP lanes for 151 cycles from both ends of the fragments on a NovaSeq 6000. Salmon (v1.4.0) [22] was used to quasi-map reads to the National Center for Biotechnology Information's *Mus musculus* Annotation Release 109 transcriptome using GRCm39 genome as the decoy sequence and options –seqBias –gcBias –numBootstraps = 30 -validateMappings. Gene-level counts were then estimated based on transcript-level counts using the "bias corrected counts without an offset" method from the tximport package [23] in R (v4.1.0). The detection threshold was set at 0.5 cpm (counts per million) in at least four samples, which resulted in 24,891 genes being filtered out, leaving 14,362 genes to be analyzed for differential expression. After filtering, the trimmed mean of M (TMM) normalization was performed and normalized log2-based cpm values (logCPM) were calculated using edgeR [24]. Differential gene expression analysis was performed using the limma-trend method [25] using a model of Group + Date. Date was considered for sample batch effect. A global false discovery rate (FDR) correction was done across all contrasts at once so that the same raw *P*-value in any contrast ends up with the same FDR *P*-value. Threshold of 0.05 was setup for global FDR correction.

Quantitative PCR analysis

Total RNA was isolated from in vivo or in vitro mice samples using a RNeasy Mini kit from Qiagen according to the manufacturer's protocol as routinely performed in our laboratory [21]. Total RNA (100 or 200 ng) was reverse transcribed according to the manufacturer's protocol using the iScript RT kit from Bio-Rad Laboratories, Inc. All samples were diluted to 1.67 ng/μL for quantitative real-time polymerase chain reactions (qPCR). The AriaMx Real-Time PCR system and the comprehensive data analysis software were used in this study. Data were generated using the TaqMan Gene Expression Master Mix (Invitrogen Life Technologies, Inc.) reagents. The expression was analyzed by using 20XTaqMan Gene Expression Assay primers (Table 1) from Applied Biosystems (Foster City, CA). The thermal cycling steps: 2 min at 50 °C to permit AmpErase uracil-N-glycosylase optimal activity, a denaturation step for 10 min at 95 °C, 15 s at 95 °C and 1 min at 60 °C for 50 cycles, followed by 1 min at 95 °C, 30 s at 58 °C, and 30 s at 95 °C for ramp dissociation. The relative amount of mRNA in each sample was calculated following the 2-$\Delta\Delta$CT method and normalized to ribosomal protein L32 (*Rpl32*).

Western blot analysis

From mouse ovarian tissues, whole-cell extracts were isolated by adding cell lysis buffer (50 mM Tris; pH 8.0, 150 mM NaCl, 1% Triton X-100, and 1 mM EDTA). Protein quantification were done using Pierce detergent compatible Bradford assay reagent (Thermo Fisher Scientific, IL) and then sample buffer (x2) was added and denatured at 95°C for 5 min. Proteins (20 μg) were separated by 12.0%

Table 1. TaqMan primers used for quantitative PCR

Genes	Assay ID	Accession no.
Rpl32	Mm02528467_g1	NM_172086.2
Nts	Mm00481140_m1	NM_024435.2
Ntsr1	Mm00444459_m1	NM_018766.2
Sort1	Mm00490905_m1	NM_001271599.1
Ptgs2	Mm00478374_m1	NM_011198.4
Pgr	Mm00435628_m1	NM_008829.2
Ell2	Mm01352835_m1	NM_138953.2
Rsad2	Mm01287122_m1	NM_021384.4
Vps37a	Mm00712884_m1	NM_033560.3

sodium dodecyl sulfate-polyacrylamide gel electrophoresis (SDS-PAGE) and subsequently transferred to nitrocellulose membranes. Membranes were blocked for 1 h at room temperature in TBST (25 mM Tris, 137 mM NaCl, 2.7 mM KCl, and 0.05% TWEEN-20) containing 5% low-fat milk and then incubated overnight at 4 °C with 1:1000 mouse anti-NTSR1 (Santa Cruz Biotechnology Cat# sc-374492, RRID:AB_10989085 [26]), 1:1000 mouse anti-SORT1 (Abcam Cat# ab16640, RRID:AB_2192606 [27]), and 1:2000 rabbit anti-BACT (Cell Signaling Technology Cat# 4970, RRID:AB_2223172 [28]) in 1% low-fat milk. The membranes were incubated with the respective secondary horseradish peroxidase–conjugated antibody for 1 h. A chemiluminescent signal was generated with the Amersham ECL Prime Western blotting detection reagent and the signal was captured using ChemiDoc (Bio-Rad Laboratories, CA).

Progesterone (P4) assay

The concentration of progesterone was measured using an Immulite kit (Diagnostic Products, CA) as described previously [19, 20]. Assay sensitivity for the Immulite was 0.02 ng/mL. The intra- and inter-assay coefficients of variation were 7 and 12%, respectively.

MTS assay

The cell metabolic activity was measured using the CellTiter 96 Aqueous One Solution MTS assay according to the manufacturer's protocol (Promega). In a 48-well dish, 50,000 cells were plated and immediately transfected with scrambled siRNA (si-NC) or siRNA targeting Nts (si-Nts) for 3 h. Then, cells were treated with or without hCG (1 IU/mL) for additional 24 h. At the end of culture, 40 μL of MTS reagent was pipetted into each well and then further incubated for an additional 2 h. The absorbance was measured at 490 nm in an Infinite F200 plate reader (Tecan) to determine the formazan concentration.

Statistical analysis

Data are presented as means ± SEM. Statistical analyses were performed using one-way analysis of variance (ANOVA) to test differences among treatments as appropriate. Tukey's post-hoc test was performed in order to identify significant differences among treatments. Means were compared with $P \leq 0.05$ considered significant. Statistical analysis was performed using GraphPad Prism (GraphPad 9, La Jolla, CA).

A.
Whole Ovary
In vivo

B.
Granulosa cells
In vivo

C.
Granulosa cells
In vitro
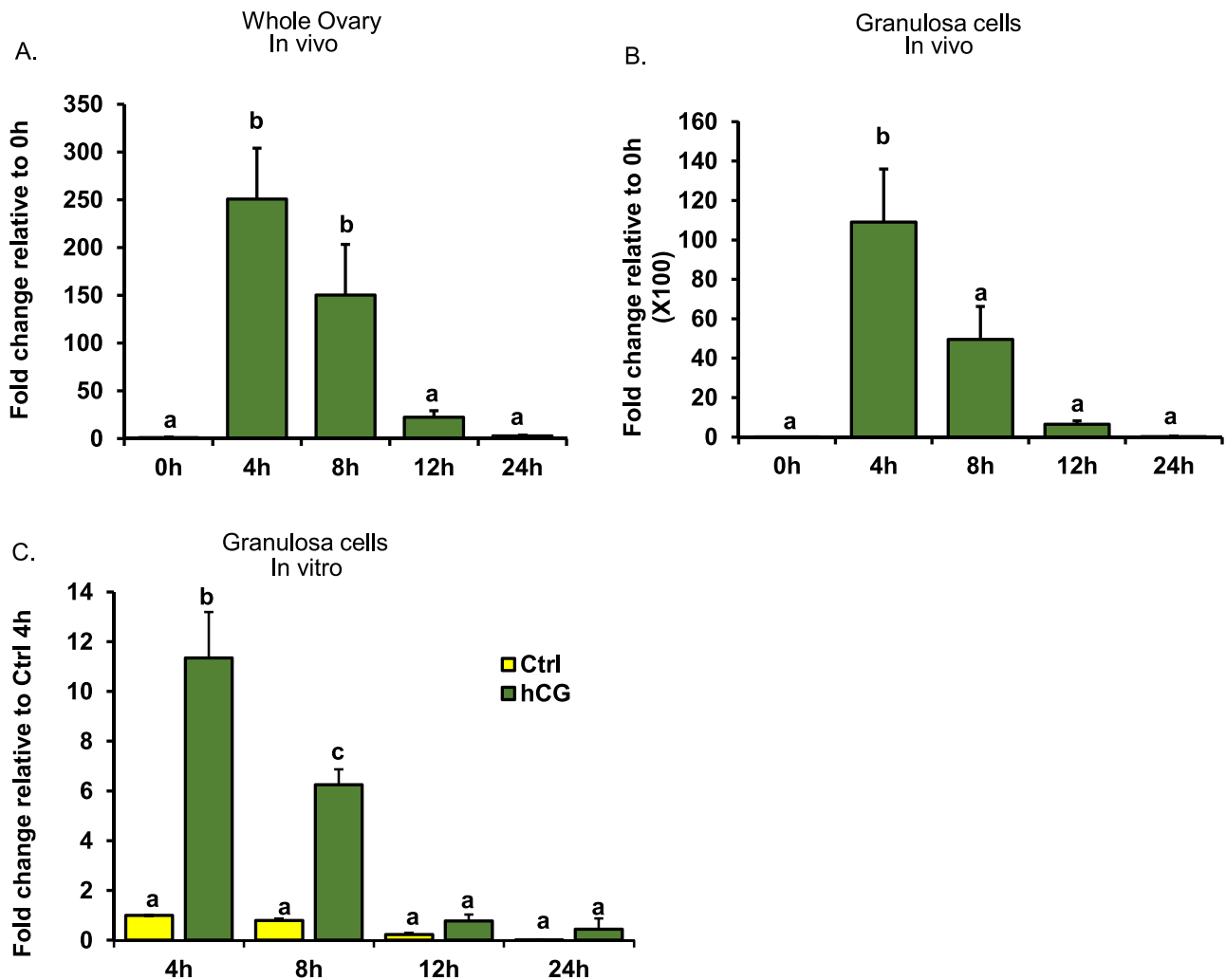
Figure 1. Expression of *Nts* across the periovulatory period. Expression of *Nts* mRNA levels in mouse ovaries (A), in mouse granulosa cells in vivo (B), and cultured mouse granulosa cells in vitro (C) following hCG administration. Results are the means ± SEM. $N = 4$. Bars that do not share a letter designation are significantly different ($P < 0.05$).

RESULTS

hCG increases *Nts* mRNA expression in vivo and in vitro

Expression of *Nts* was examined in whole ovaries collected across the periovulatory period. The expression of *Nts* increased approximately 250-fold at 4 h after hCG which remained elevated until 8 h post-hCG, then the mRNA levels gradually declined back to baseline at 24 h after hCG ($P > 0.05$; Figure 1A). Next, we examined the in vivo expression of *Nts* in mouse granulosa cells. Similar to our findings from the whole ovary, *Nts* expression displayed a similar pattern in mouse granulosa cells, with an induction of *Nts* by hCG at 4 h and levels declining throughout the late periovulatory period (Figure 1B). To determine the granulosa cell contribution of *Nts* expression observed in whole ovaries, *Nts* expression was directly compared in whole ovaries and granulosa cells at 4 h after hCG. The *Nts* mRNA levels in granulosa cells were approximately 8-fold higher at 4 h after hCG than in whole ovaries. The lowest level of detection for *Nts* expression was 35 Ct values in whole ovaries and in vivo granulosa cells, which was within the linear range of the qPCR assay. We also found a similar pattern of *Nts* induction

by hCG treatment in cultured granulosa cells. As shown in Figure 1C, hCG upregulated *Nts* at 4 h and the induction remained elevated at 8 h, confirming that the induction of *Nts* mRNA levels in cultured granulosa cells is similar to that in granulosa cells of the periovulatory follicle in vivo.

Expression of Nts receptors across the periovulatory period

The expression of the three different known NTS receptors designated as *Ntsr1*, *Ntsr2*, and *Sort1* was determined in mouse ovaries and granulosa cells in order to better understand how NTS conveys its function in the ovary. In intact ovaries, expression of *Ntsr1* did not change with hCG treatment (Figure 2A). *Ntsr2* had cycle threshold values above 40 cycles, indicating low levels of expression. *Ntsr2* expression did not change with hCG treatment (data not shown). As shown in Figure 2B, *Sort1* expression decreased over the ovulatory period with the lowest levels at 24 h. When confirming the protein levels of NTSR1 and SORT1, we found that the protein levels were unchanged across the periovulatory period (Figure 2C and D, respectively). Similarly, in granulosa cells collected across the periovulatory period, expression of *Ntsr1*
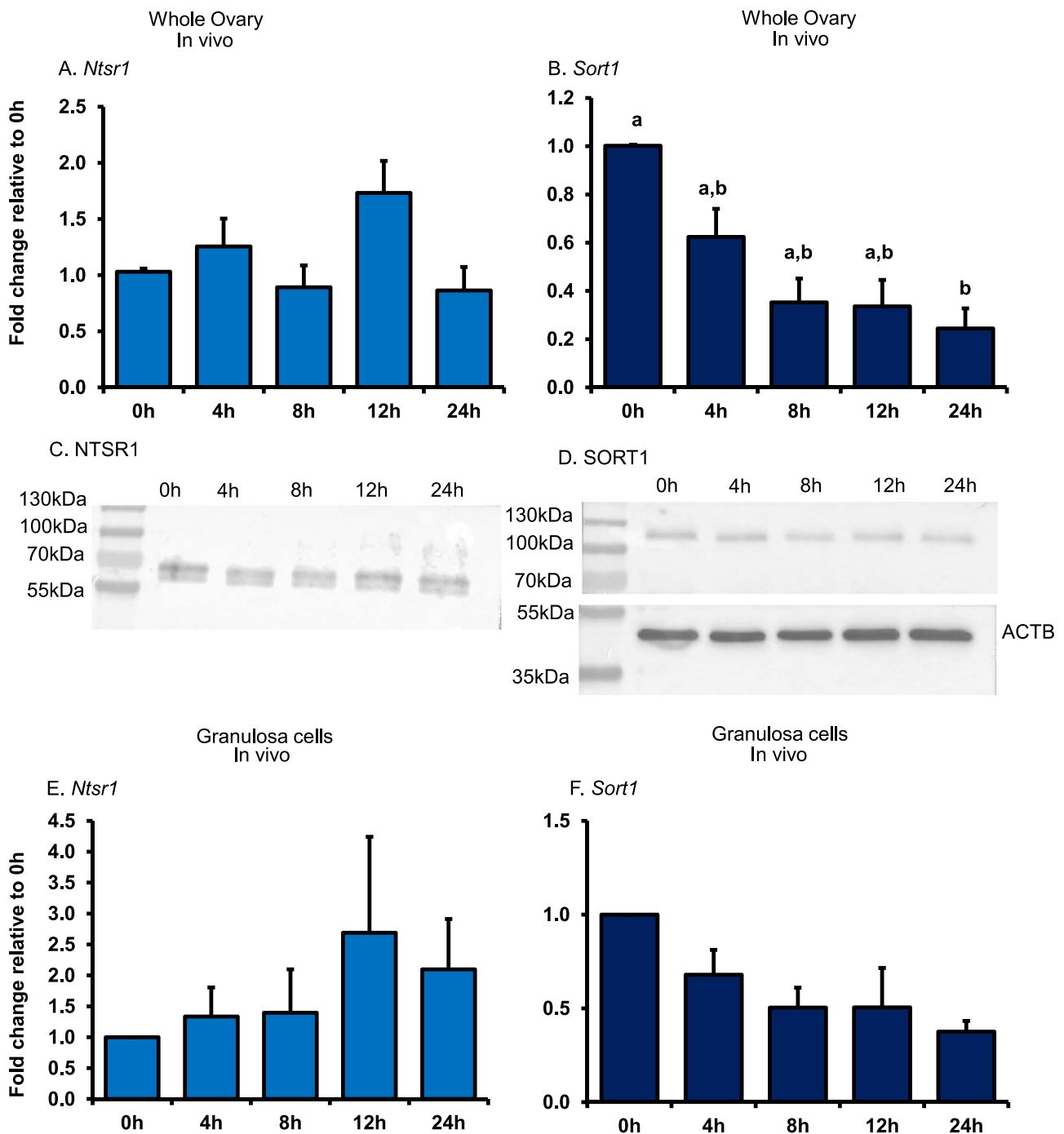
Figure 2. Expression of Nts receptors across the periovulatory period. The expression of *Ntsr1* (A) and *Sort1* (B) in mouse ovaries collected after hCG is shown. Western blots illustrate representative protein bands of NTSR1 (C), and SORT1 and b-actin (ACTB, D) in mouse ovaries. The expression of *Ntsr1* (E) and *Sort1* (F) in granulosa cells collected across the periovulatory period is depicted. Results are the means ± SEM. $N = 4$. Bars that do not share a letter designation are significantly different ($P < 0.05$).

(Figure 2E) did not change, whereas *Ntsr2* was not detectable (data not shown). Also, *Sort1* expression in mouse granulosa cells in vivo tended to decline but was not statistically different over the periovulatory period (Figure 2F).

Regulation of hCG-induced *Nts* expression in mouse granulosa cells

To understand the regulatory mechanism underlying *Nts* expression, granulosa cells were treated in vitro with specific inhibitors of hCG-activated signaling pathways in the presence and absence of hCG. As shown in Figure 3, *Nts* mRNA levels were increased by hCG treatment. Concomitant treatment with hCG and H89 (a PKA inhibitor) or SB (p38MAPK inhibitor) suppressed the hCG-induced *Nts* expression (Figure 3). These results indicate that the PKA pathway and p38MAPK are involved in hCG-induced upregulation of *Nts* expression in mouse granulosa cells.

Next, to study the role of LH/hCG-induced paracrine mediators regulating *Nts* expression, granulosa cells were cultured with inhibitors of the major LH/hCG signaling
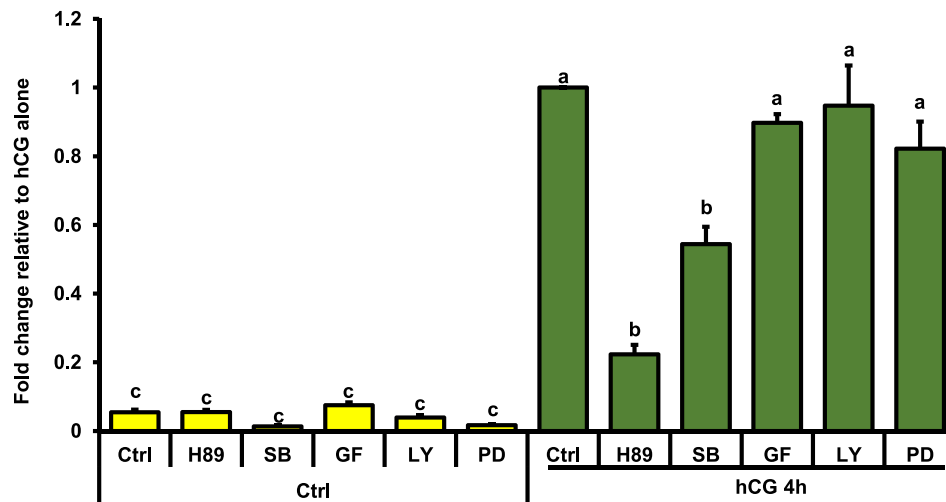
Figure 3. Effect of inhibitors on the hCG-induced increase in *Nts* expression in mouse granulosa cells in vitro. Granulosa cells were preincubated for 1 h with the following signaling inhibitors of hCG: H89 (PKA inhibitor), SB (SB203580; p38 MAPK inhibitor), GF (GF109203x; PKC inhibitor), LY (LY294002; PI3K inhibitor), or PD (MKK/MEK inhibitor). Cells were then treated with or without hCG treatment (1 IU/mL) for 4 h. Results are the means $\pm$ SEM. $N = 6$. Bars that do not share a letter designation are significantly different ($P < 0.05$).
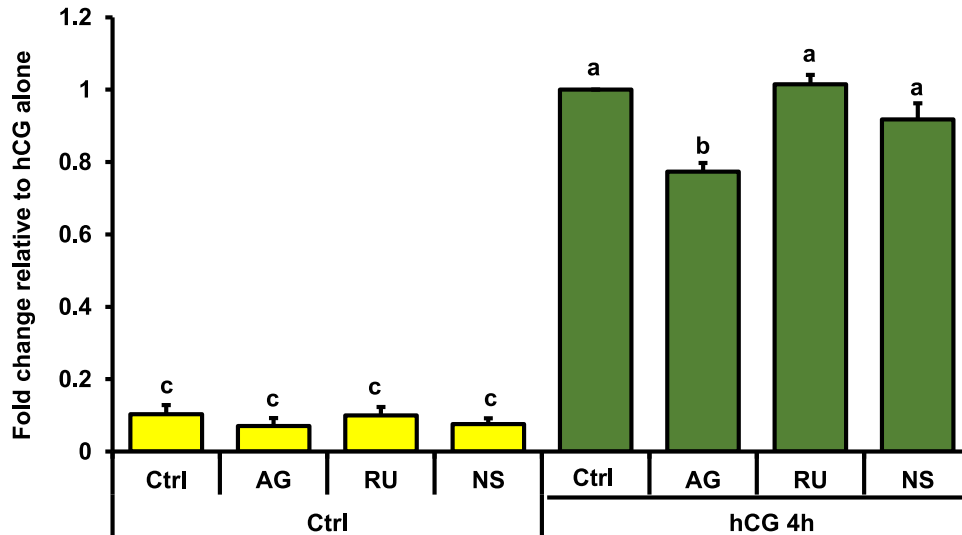
Figure 4. Effect of hCG-induced signaling pathway inhibitors on the regulation of *Nts* expression in mouse granulosa cells in vitro. Inhibitors for the hCG signaling pathways were used to determine which signaling pathways are involved in the expression of *Nts*. Granulosa cells were preincubated for 1 h with the following hCG pathway inhibitors: AG (AG1478; EGF receptor inhibitor), RU (RU486; progesterone receptor antagonist), and NS (NS398; prostaglandin synthase 2 inhibitor). Cells were then treated with or without hCG treatment (1 IU/mL) for 4 h. Results are the means $\pm$ SEM. $N = 7$. Bars that do not share a letter designation are significantly different ($P < 0.05$).

pathways such as the progesterone, prostaglandin, and the epidermal growth-like factor (EGF) pathways in presence and absence of hCG. *Nts* mRNA expression was induced by hCG and this induction was partially blocked by the EGF receptor inhibitor AG1478 in granulosa cells (Figure 4). This implies that *Nts* expression is also regulated via EGF receptor signaling. Furthermore, P4 levels were unchanged in the culture media treated with above-mentioned inhibitors, however, as expected hCG treatment increased P4 levels (Supplementary Figure 1).

Effect of *Nts* knockdown in mouse granulosa cells

To examine the potential role of NTS during the ovulatory period, gene knockdown in mouse granulosa cells with small interfering RNA was employed. As expected, hCG treatment induced *Nts* expression at both 4 h and 12 h in the granulosa

cells transfected with si-NC (Figure 5). Strikingly, in the granulosa cells transfected with si-Nts and treated with hCG for 4 h and 12 h, we observed by qPCR that *Nts* mRNA levels were reduced 75% and 90%, respectively, compared to *Nts* mRNA levels in granulosa cells treated with si-NC and hCG (Figure 5). Furthermore, P4 levels were unchanged in the culture media treated with si-NC or si-Nts, however, as expected hCG treatment increased P4 levels (Supplementary Figure 2).

Then, to identify RNA transcripts impacted by Nts silencing an RNAseq approach was utilized. Total RNA samples isolated from three groups (si-NC-Ctrl, si-NC-hCG, si-Nts-hCG) at 4 h and 12 h post hCG were subjected to RNA-seq ($n = 4$). The complete dataset was submitted to the Gene Expression Omnibus (accession GSE210811). A total of 60 genes were listed to be differentially expressed genes (DEGs) among which 43 were decreased in si-Nts-hCG vs si-NC-hCG,

A.

B.
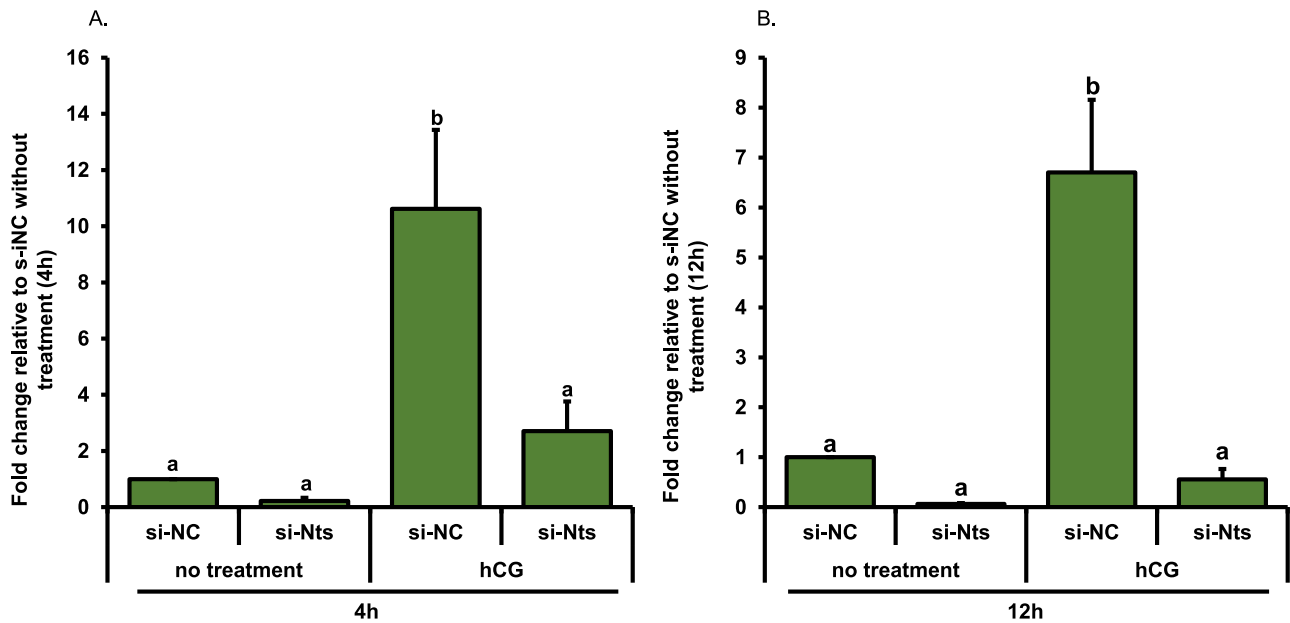
Figure 5. Effect of *Nts* gene knockdown by siRNA targeting *Nts* in mouse granulosa cells. Cells were transfected with scrambled siRNA (control; si-NC) or siRNA targeting *Nts* (si-Nts). After 3 h of transfection, cells were treated with or without hCG (1 IU/mL) for another 4 h (A) and 12 h (B). The expression of *Nts* mRNA after *Nts* knockdown is shown. Results are the means ± SEM. $N = 4$. Bars that do not share a letter designation are significantly different ($P < 0.05$).

whereas 17 genes were increased in si-Nts-hCG vs si-NC-hCG at 4 h based on a selection criteria logCPM > 0.05, and false discovery rate < 0.05 (Figure 6A and Supplementary Table 1). A heatmap showed similarity and repeatability in the gene expression of each treatment group and stark differences between treatments (Figure 6B). In addition, a total of 3961 genes were regulated by hCG treatment at 4 h. Of the DEGs 2291 were decreased and 1670 genes were increased, respectively in the si-NC-hCG vs si-NC-Ctrl at 4 h treatment groups (Supplementary Table 1).

We next examined genes that were regulated by hCG treatment at 12 h. A total of 3521 genes were listed to be differentially expressed. Among 3521 DEGs,1722 genes were decreased and 1799 genes were increased, respectively in the si-NC-hCG vs si-NC-Ctrl treatment groups at 12 h based on a selection criteria logCPM > 0.05, and false discovery rate < 0.05 (Supplementary Table 2). Then, we examined the genes differentially regulated by silencing *Nts*. With the same selection criteria in si-NTS-hCG vs si-NC-hCG at 12 h groups, 331 genes were listed to be differentially expressed in si-NTS-hCG vs si-NC-hCG, (Supplementary Table 2). Of the DEGs, 209 and 122 genes were decreased and increased, respectively, in siNTS-hCG compared with the siNC-hCG treatment (Figure 7A and Supplementary Table 2). A heatmap showed similarity and repeatability in the gene expression of each treatment group and stark differences between treatments (Figure 7B). Among the 209 DEGs, 39 genes that were downregulated in *Nts* silenced granulosa cells were found to be upregulated by hCG, implying that these genes could be regulated by NTS in mouse granulosa cells (Table 2). In addition, among the 122 DEGs that were upregulated in granulosa cells treated with si-NTS-hCG, 33 genes were suppressed by hCG treatment (Table 2). This demonstrates that genes suppressed by LH/hCG during ovulation are also regulated by NTS as knocking down *Nts* expression lead to increased expression of these genes.

We next examined a select few of these downregulated genes to confirm the RNAseq findings. As shown in Figure 8A–C, the expression of elongation factor for RNA polymerase II 2 (*Ell2*), radical S-adenosyl methionine domain containing 2 (*Rsad2*), and vacuolar protein sorting 37A (*Vps37a*), respectively, were confirmed by qPCR to be induced by hCG treatment and strongly decreased by knocking down *Nts* expression. In addition, smoothelin-like 2 (Smtnl2) was reduced by hCG treatment and strongly increased by knocking down *Nts* expression (Figure 8D). These qPCR data thereby confirm the RNAseq results. In addition, expression of prostaglandin synthase 2 (*Ptgs2*) and progesterone receptor (*Pgr*) were unchanged in *Nts* silenced cells (Figure 8E and F), implying that these two major LH-induced paracrine factors are not regulated by NTS.

Effect of *Nts* knockdown on mouse granulosa cell metabolism

To determine whether the knock-down of *Nts* expression in mouse granulosa cells resulted in any functional changes, cell metabolic activity was assessed. Cells were transfected with siNC as a control or si-Nts to knockdown *Nts* expression and then treated with or without hCG (1 IU/ml). The metabolic activity of granulosa cells was evaluated using the MTS assay. As shown in Figure 9, MTS values were increased by knocking down *Nts* expression alone. As expected, hCG treatment increased the MTS values, however hCG treatment masked the effect of *Nts* knockdown (Figure 9). This demonstrates that NTS may inversely regulate cell metabolic activity.

Discussion

The present findings characterize the induction, regulation, and function of NTS during the periovulatory period in the mouse ovary. The hCG-induced expression of *Nts* is
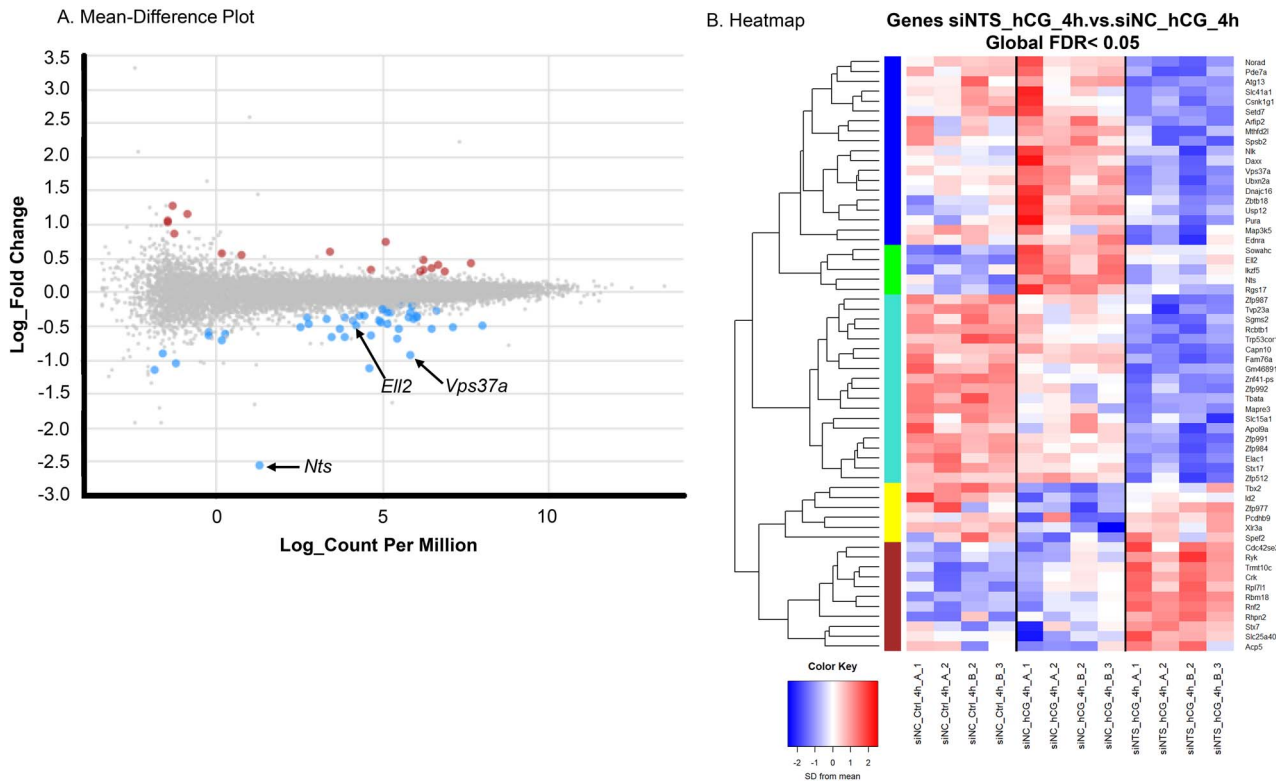
Figure 6. RNA-seq analysis using primary mouse granulosa cells transfected with si-NC or si-NTS and treated with or without hCG for 4 h. High-throughput RNA-seq analysis was performed using mouse granulosa cells obtained from four replicates (one replicate contains pooled granulosa cells from three mice). The cells were transfected with si-NC (negative control) or si-Nts (siRNA specific to mouse *Nts*) and treated with or without hCG (1 IU/mL) for 4 h. (A) Mean-difference (MD) plot displays gene-wise log2-fold changes against average expression values together with a plot of sample expression. Dots in red, gray, and blue represent genes that show an increase, no change, or a decrease in expression values by the knockdown of *Nts* with hCG treatment, respectively. Arrows point to select specific genes that are decreased by *Nts* silencing that were further analyzed. (B) The heatmap indicates the group difference of DEGs between si-NC-Ctrl (no treatment), si-NC-hCG, and si-NTS-hCG treated mouse granulosa cells and the repeatability within each group. Thresholds used in MD plot and heatmap were FDR < 0.05 to select DEGs between the groups.

robust in granulosa cells. This *Nts* expression is regulated through classical hCG signaling pathways acting, in part, through the EGF receptor signaling pathway. The receptors for NTS show different patterns of mRNA expression with only *Sort1* decreasing after hCG. However, the protein levels of NTSR1 and SORT1 remained unchanged across the periovulatory period. Using a siRNA approach in combination with RNAseq, several genes such as *Ell2*, *Rsad2*, *Vps37a*, and *Smtnl2* were identified as downstream genes of NTS. Moreover, knocking down *Nts* lead to increased cell metabolic activity implying that NTS could be acting as regulator of granulosa cell activity. These data provide new insight into the potential role of NTS during the periovulatory period.

In the current study, there is a rapid increase in *Nts* in granulosa cells within 4 h after hCG administration. These findings are similar to previous studies reporting a striking hCG-induced *NTS* mRNA expression in rat, human, and non-human primate granulosa cells [2, 3]. Furthermore, as demonstrated by immunolocalization of NTS in the both the human and non-human primate, hCG also induced NTS protein in granulosa cells [2, 3]. These studies establish that administration of hCG in vivo, to mimic the ovulatory LH surge, results in *Nts* stimulation in granulosa cells across the mouse, rat, non-human primate, and the human ovary. In addition, hCG-induced *Nts* expression was found to be regulated similarly across these species. In the present study, *Nts* mRNA is induced by hCG through the classical signaling

pathways such as the PKA and p38MAPK pathways in mouse granulosa cells. Likewise, in the human and rat, hCG-induced *NTS* expression through the PKA, PKC, and MAPK signaling pathways [2]. There are, however, slight species differences in the hCG-induced *Nts* expression in granulosa cells. In the rat, PI3 kinase and MEK1/2 ERK1/2 signaling pathways were also shown to regulate hCG-induced *Nts* expression in granulosa cells [2]. Nonetheless, hCG induces *Nts* expression in granulosa cells via the cAMP-dependent PKA pathway which appears to be a major common signaling pathway in the mouse, rat, and human ovary.

Another major LH/hCG-induced paracrine signaling pathway regulating NTS expression in the granulosa cells appears to be the EGF receptor signaling pathway [19]. Inhibition of the EGF signaling pathway results in a partial decrease in NTS mRNA in mouse granulosa cells in the present study which is similar to previous findings in the rat and human [2]. Likewise, in mouse cumulus cells EGF upregulated *Nts* mRNA levels and inhibition of MAPK kinase by using U0126 decreased the EGF-induced *Nts* expression [8]. The current findings in the mouse align with previous studies that have demonstrated an EGF regulation of NTS expression.

NTS conveys its action through its three receptors characterized as NTSR1, NTSR2, and SORT1 [14, 29]. In this study, the expression of *Ntsr1* and *Ntsr2* were extremely low and did not change with hCG treatment. Moreover, *Ntsr2* was barely detectable in the mouse ovary and in granulosa

Table 2. List of differentially regulated genes by *Nts* knockdown in mouse granulosa cells

S.N.	Gene	ENTREZID	Product	logFC (differentially regulated genes by silencing Nts)	logFC (differentially regulated by hCG treatment)
1	*Nts*	67405	Neurotensin	−3.095	3.529
2	*Rsad2*	58185	Radical S-adenosyl methionine domain containing 2	−1.541	1.467
3	*Vps37a*	52348	Vacuolar protein sorting 37A	−1.204	0.6323
4	*Ell2*	192657	Elongation factor for RNA polymerase II 2	−0.9541	0.7553
5	*Ubxn2a*	217379	UBX domain protein 2A	−0.8576	0.3915
6	*Rgs9*	19739	Regulator of G-protein signaling 9, transcript variant 2	−0.8037	0.7638
7	*Rtn4r*	65079	Reticulon 4 receptor	−0.7779	0.6655
8	*Adrb2*	11555	Adrenergic receptor, beta 2	−0.7762	1.481
9	*Pdap1*	231887	PDGFA associated protein 1, transcript variant 1	−0.7598	0.4641
10	*Gpr20*	239530	G protein-coupled receptor 20	−0.7294	0.6305
11	*Usp12*	22217	Ubiquitin specific peptidase 12	−0.7231	0.4879
12	*Rgs17*	56533	Regulator of G-protein signaling 17, transcript variant 2	−0.6979	1.077
13	*Ccn4*	22402	Cellular communication network factor 4, transcript variant 1	−0.6288	1.108
14	*Clcn5*	12728	Chloride channel, voltage-sensitive 5, transcript variant X6	−0.581	0.6205
15	*Ddx19a*	13680	DEAD box helicase 19a	−0.5521	0.5259
16	*Pag1*	94212	Phosphoprotein associated with glycosphingolipid microdomains 1, transcript variant A	−0.5279	0.6528
17	*Klhl29*	208439	Kelch-like 29	−0.5108	0.6688
18	*Mrpl19*	56284	Mitochondrial ribosomal protein L19	−0.47	0.4783
19	*E2f2*	242705	E2F transcription factor 2, transcript variant 2	−0.4693	1.032
20	*Podxl*	27205	Podocalyxin-like	−0.4504	0.4518
21	*Selenoi*	28042	Selenoprotein I, transcript variant 1	−0.4253	0.7486
22	*Sowahc*	268301	Sosondowah ankyrin repeat domain family member C	−0.4225	0.4111
23	*Il6ra*	16194	Interleukin 6 receptor, alpha, transcript variant 2	−0.3899	0.806
24	*Actr2*	66713	ARP2 actin-related protein 2, transcript variant 2	−0.3885	0.3328
25	*Zfp983*	73229	Zinc finger protein 983, transcript variant X1	−0.3881	0.5492
26	*Pdp2*	382051	Pyruvate dehydrogenase phosphatase catalytic subunit 2	−0.3822	0.4902
27	*Pank1*	75735	Pantothenate kinase 1, transcript variant 1	−0.3797	0.2563
28	*Wdr4*	57773	WD repeat domain 4	−0.3719	0.3496
29	*Tpcn1*	252972	Two pore channel 1	−0.3671	0.356
30	*Ankrd46*	68839	Ankyrin repeat domain 46, transcript variant 3	−0.3472	0.6282
31	*Slc6a6*	21366	Solute carrier family 6 (neurotransmitter transporter, taurine), member 6	−0.3454	1.18
32	*Cul2*	71745	Cullin 2, transcript variant 2	−0.3231	0.3792
33	*Layn*	244864	Layilin, transcript variant X1	−0.3187	0.6605
34	*Ttc9*	69480	Tetratricopeptide repeat domain 9	−0.2934	1.039
35	*Stx3*	20908	Syntaxin 3, transcript variant A	−0.2747	0.3696
36	*Tmem87b*	72477	Transmembrane protein 87B, transcript variant 2	−0.2411	0.2479
37	*Stk38l*	232533	Serine/threonine kinase 38 like, transcript variant 1	−0.2354	0.4117
38	*Acadsb*	66885	Acyl-Coenzyme A dehydrogenase, short/branched chain	−0.2188	0.359
39	*Brox*	71678	BRO1 domain and CAAX motif containing, transcript variant 1	−0.1811	0.3339
40	*Smtnl2*	276829	Smoothelin-like 2	1.229	−2.759
41	*Bend5*	67621	BEN domain containing 5, transcript variant 1	0.7233	−1.076
42	*Sox13*	20668	SRY (sex determining region Y)-box 13, transcript variant X5	0.7226	−1.174
43	*Ptprr*	19279	Protein tyrosine phosphatase, receptor type, R, transcript variant 3	0.7213	−2.253
44	*Rims1*	116837	Regulating synaptic membrane exocytosis 1, transcript variant 5	0.7154	−1.432
45	*Sox18*	20672	SRY (sex determining region Y)-box 18	0.6962	−1.331
46	*Cpox*	12892	Coproporphyrinogen oxidase	0.6795	−0.3989

Table 2. Continued.

S.N.	Gene	ENTREZID	Product	logFC (differentially regulated genes by silencing Nts)	logFC (differentially regulated by hCG treatment)
47	*Tmem143*	70209	Transmembrane protein 143	0.6704	−0.4108
48	*Dlc1*	50768	Deleted in liver cancer 1, transcript variant 2	0.6351	−0.7031
49	*Ssx2ip*	99167	Synovial sarcoma, X 2 interacting protein, transcript variant 1	0.6343	−0.682
50	*Fos*	14281	FBJ osteosarcoma oncogene	0.5989	−0.4406
51	*Phlda1*	21664	Pleckstrin homology like domain, family A, member 1	0.5458	−1.19
52	*Tcim*	69068	21	0.5347	−0.5192
53	*Traf5*	22033	TNF receptor-associated factor 5	0.5276	−1.131
54	*Igsf9*	93,842	Immunoglobulin superfamily, member 9, transcript variant 2	0.5177	−1.16
55	*Rcan2*	53901	Regulator of calcineurin 2, transcript variant 1	0.5102	−2.087
56	*Tnfrsf21*	94185	Tumor necrosis factor receptor superfamily, member 21	0.4713	−0.5271
57	*Msrb3*	320183	Methionine sulfoxide reductase B3	0.4608	−1.493
58	*Sh3bp4*	98402	SH3 domain-binding protein 4	0.4512	−0.7327
59	*Prkacb*	18749	Protein kinase, cAMP dependent, catalytic, beta, transcript variant 1	0.3677	−0.3108
60	*Rhobtb3*	73296	Rho-related BTB domain containing 3	0.3559	−0.6639
61	*Lpcat1*	210992	Lysophosphatidylcholine acyltransferase 1, transcript variant 1	0.3524	−0.2755
62	*Fam122b*	78755	Family with sequence similarity 122, member B, transcript variant X6	0.334	−0.6991
63	*Egr1*	13653	Early growth response 1	0.3185	−0.3997
64	*Cited2*	17684	Cbp/p300-interacting transactivator, with Glu/Asp-rich carboxy-terminal domain, 2	0.3171	−0.4228
65	*Pawr*	114774	PRKC, apoptosis, WT1, regulator, transcript variant X1	0.3146	−0.4884
66	*Rbpms*	19663	RNA-binding protein gene with multiple splicing, transcript variant 2	0.2992	−0.6444
67	*Fbxo21*	231670	F-box protein 21, transcript variant 2	0.2959	−0.445
68	*Rbpj*	19664	Recombination signal binding protein for immunoglobulin kappa J region, transcript variant 2	0.275	−0.5301
69	*Iqcb1*	320299	IQ calmodulin-binding motif containing 1	0.2639	−0.4641
70	*Mex3d*	237400	mex3 RNA-binding family member D	0.2438	−0.3742
71	*Fgfrl1*	116701	Fibroblast growth factor receptor-like 1, transcript variant 1	0.2298	−0.6631
72	*Dbn1*	56320	Drebrin 1, transcript variant 3	0.2239	−0.7216
Legend		🟩	*hCG-upregulated genes whose mRNA levels are reduced by NTS silencing*		
		🟧	*hCG-downregulated genes whose mRNA levels are increased by NTS silencing*		

cells. This expression pattern is similar to findings in human and monkey granulosa cells where expression of *NTSR1* and *NTSR2* mRNA was extremely low in the human [2] and in the monkey, *NTSR2* was low while *NTSR1* mRNA was undetectable [3]. However, there were species differences in the hCG-induced regulation of NTSR1 and NTSR2. In human granulosa cells collected across the periovulatory period, NTSR2 decreased approximately 80% after hCG administration during the preovulatory period [2], whereas NTSR2 was unchanged in monkey granulosa cells [3]. Unlike NTSR1 and NTSR2, the expression of SORT1 was abundant in mouse granulosa cells in the present study and in rat and human granulosa cells [2]. Although species differences were noted in the hCG regulation of SORT1 [3], in all species SORT1 was found to be the only NTS receptor mRNA that is highly expressed in granulosa cells even though the protein levels were unchanged. However, the role of the NTSR1 and NTSR2 in NTS action cannot be underestimated even though

their mRNA expression levels were low in the granulosa cells. For example, NTSR1 and SORT1 are the prominent NTS receptors reported in certain cancers, such as pancreatic cancer and human colorectal cancer [30, 31], suggesting that these receptors could act as potential progressive biomarkers or pharmacological targets for novel therapies targeting the neurotensinergic pathways. A study of ovarian cancer cells showed that blockade of NTSR1 with an antagonist reduced cell proliferation but increased cell migration, whereas knockdown of SORT1 mimicked the anti-proliferative effects of NTSR1 blockade on ovarian cancer cells [12]. Thus, information derived from cancer studies implies that the type of receptor may dictate NTS actions and that some of these actions of NTS, such as cell proliferation and/or cell migration, may have a role in the ovulatory process.

In the present study, a *Nts* silencing approach followed by RNAseq has revealed several genes that are regulated by NTS. Genes such as *Ell2, Rsad2, Vps37a,* and *Smtnl2* were

A. Mean-Difference Plot

B. Heatmap
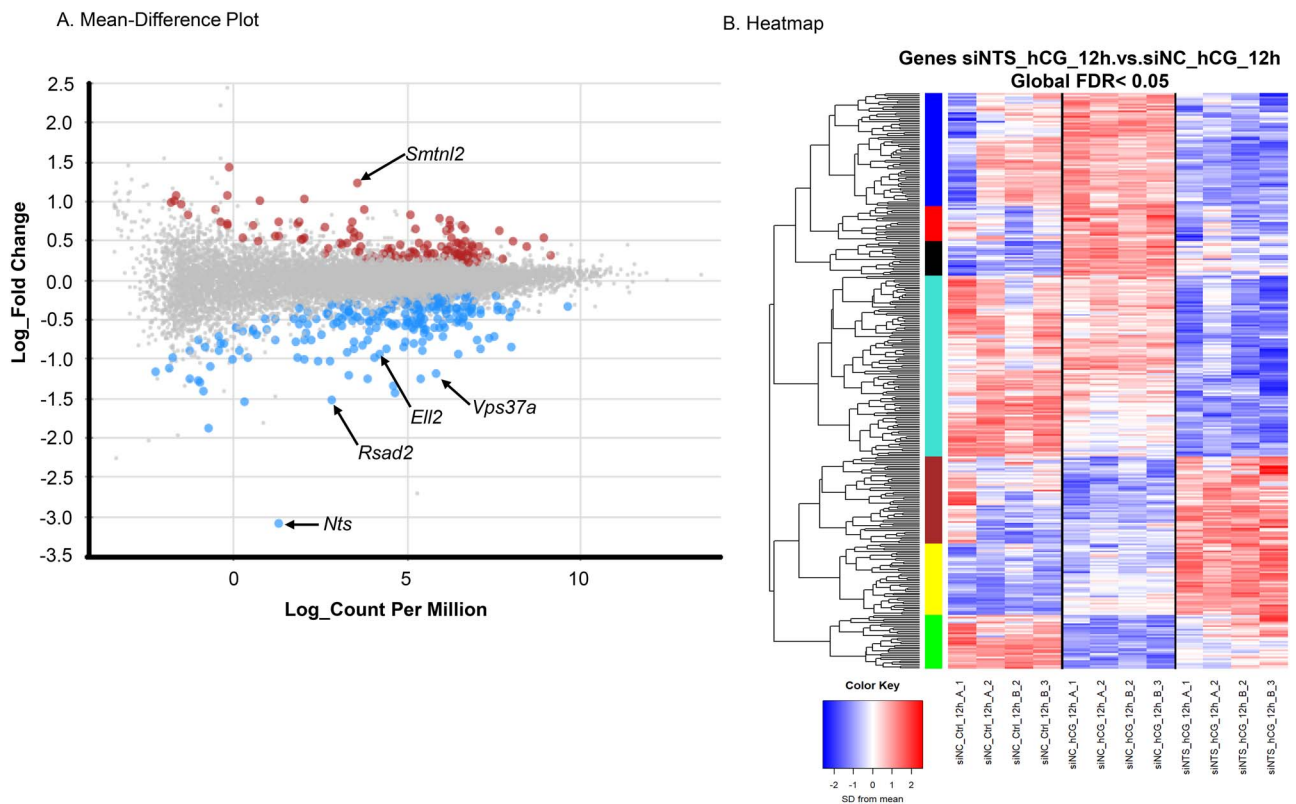
Figure 7. RNA-seq analysis using primary mouse granulosa cells transfected with si-NC or si-NTS and treated with or without hCG for 12 h. High-throughput RNA-seq analysis was performed using mouse granulosa cells obtained from four replicates (one replicate contains pooled granulosa cells from three mice). The cells were transfected with si-NC (negative control) or si-Nts (siRNA specific to mouse *Nts*) and treated with or without hCG (1 IU/mL) for 12 h. (A) Mean-difference (MD) plot displays gene-wise log2-fold changes against average expression values together with a plot of sample expression. Dots in red, gray, and blue represent genes that show an increase, no change, or a decrease in expression values by the knockdown of *Nts* with hCG treatment, respectively. Arrows point to select specific genes that are decreased by *Nts* silencing that were further analyzed. (B) The heatmap indicates the group difference of DEGs between si-NC-Ctrl (no treatment), si-NC-hCG, and si-NTS-hCG treated mouse granulosa cells and the repeatability within each group. Thresholds used in MD plot and heatmap were FDR < 0.05 to select DEGs between the groups.

found to be downstream of NTS in mouse granulosa cells. ELL2 is a member of the elongation factor component which is required to increase the catalytic rate of RNA polymerase II transcription [32, 33]. Studies using *Ell2*-knockout mice have revealed that the loss of *Ell2* results in increased epithelial proliferation and vascularity in the prostate [34] and a reduction in Ig secretion and an alteration in the expression of the unfolded protein response genes in B cells [32]. Even though the role of ELL2 in the ovary is still unknown, it is possible that in the ovary ELL2 acts as in other systems to regulate cell proliferation, vascularity, and secretion of paracrine factors, all the key attributes that promote the ovulatory process.

Radical S-adenosylmethionine domain-containing protein 2 (RSAD2; viperin) is an interferon-inducible antiviral protein which plays a major role in the cell antiviral state. RSAD2 is a key enzyme in innate immune responses and inflammatory stimuli in many cell types [35]. A recent study has shown that decreased expression of interferon-stimulated genes occurs correspondingly with the decline of antiviral innate responsiveness in the later phase of SARS-CoV-2 infection [36]. Studies have highlighted the potential impact of SARS-CoV-2 in the ovary [37–39]. It was shown that in immortalized granulosa cells (COV434) stimulated with follicular fluid obtained from post COVID-19 patients, the expression of

steroidogenic acute regulatory protein (*StAR*), estrogen-receptor *β* (*Erβ*), and vascular endothelial growth factor (*VEGF*) were significantly decreased, suggesting that SARS-CoV-2 infection adversely affects the follicular microenvironment [38]. Thus, stimulation of RASD2 either by LH or LH-induced NTS may have a protective effect against viral infection in the ovary. Moreover, in the ovary, RSAD2 induction in granulosa cells might be a self-defense mechanism to protect against viral entry into the follicle.

Vacuolar protein sorting 37 homolog A (VPS37A) is a member of the endosomal sorting complex required for the transport system involved in endocytosis [40]. Studies have demonstrated that silencing or knocking down VPS37A strongly delayed the degradation process of EGF receptor [40] and retained phosphorylated EFG receptor and hyperactivation of downstream EGF pathways [41]. These studies suggest a potential role of VPS37A in the follicle where VPS37A adjusts the signaling mechanism of paracrine factors, such as EGF signaling pathway, and might facilitate the transition of the ovulated follicle into the corpus luteum. In accord, cell metabolic activity was upregulated in *Nts* knocked down granulosa cells in the present study. In support, gene ontology analysis has shown that 68 genes involved in cellular metabolic process were influenced by *Nts* knockdown. Moreover, 56 genes involved in cellular macromolecule metabolic process
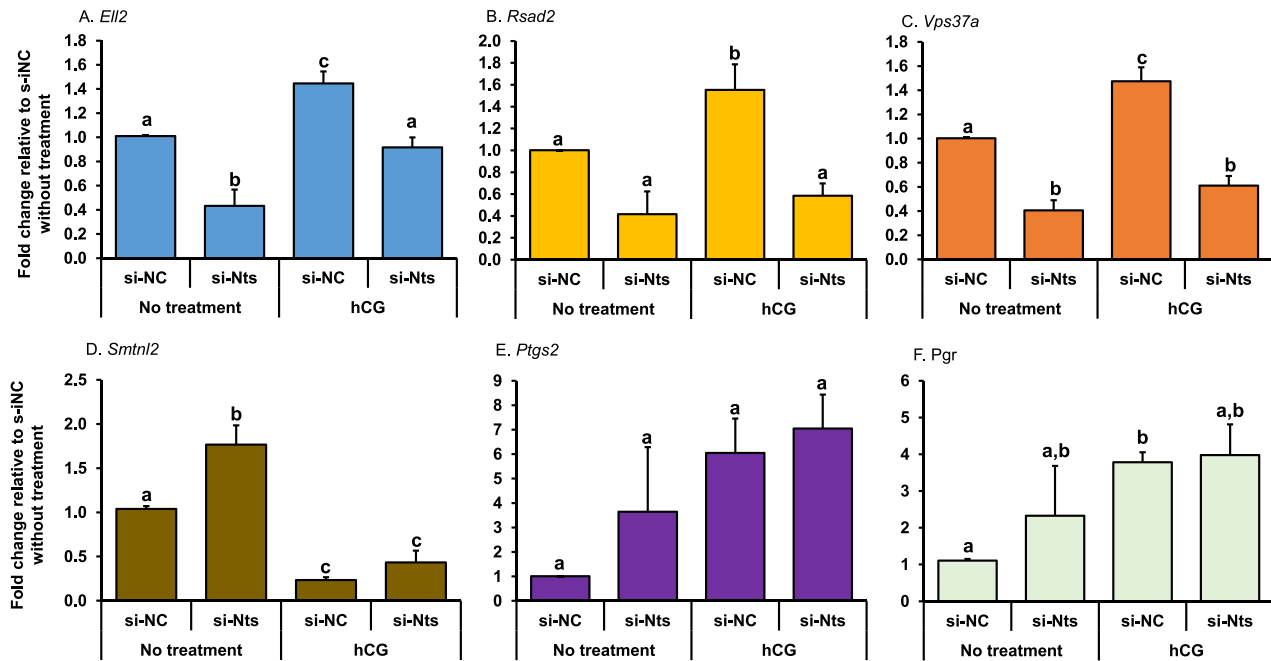
Figure 8. Effect of *Nts* gene knockdown in mouse granulosa cells. Cells were transfected with scrambled siRNA (si-NC) or siRNA targeting *Nts* (si-Nts). After 3 h of transfection, cells were treated with or without hCG (1 IU/mL) for another 12 h. The expression of (A) *Ell2* mRNA, (B) *Rsad2* mRNA, (C) *Vps37a* mRNA, (D) *Smtnl2* mRNA, (E) *Ptgs2* mRNA, and (F) *Pgr* mRNA after *Nts* knockdown is shown. Results are the means ± SEM. $N = 4$. Bars that do not share a letter designation are significantly different ($P < 0.05$).
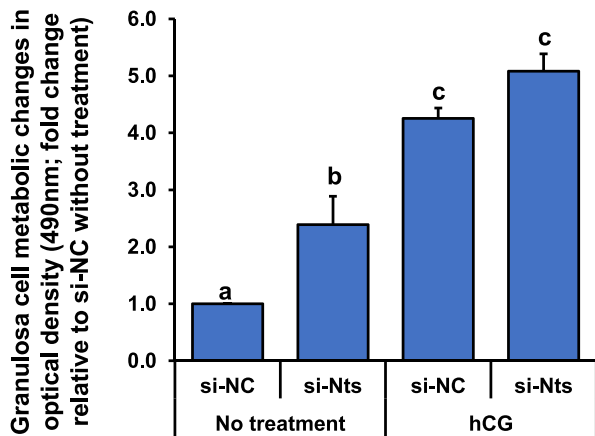
Figure 9. Effect of Nts gene knockdown on mouse granulosa cell metabolic changes. Cells were transfected with scrambled siRNA (si-NC) or siRNA targeting Nts (si-Nts). After 3 h of transfection, cells were treated with or without hCG (1 IU/mL) for 24 h. Cell metabolic activity was assessed by recording the absorbance at 490 nm using the MTS assay. The experiments were repeated in four independent batches with three replicates in each batch. Results are the means ± SEM. $N = 4$. Bars that do not share a letter designation are significantly different ($P < 0.05$).

were also affected by knocking down *Nts*. Nonetheless, studies on these genes require further research in the future. This suggests that NTS could inversely regulate cell activity supporting smooth transition of follicular cells to luteal cells.

Smoothelin-like 2 is a c-Jun N-terminal kinase substrate and acts as an actin filament-binding protein. It is expressed in skeletal muscle and is associated with differentiating myocytes [42]. Besides skeletal muscle cells, Sertoli cells in the mouse testis express *Smtnl2* [43]. Knocking down *Smtnl2* expression disrupted spermatogenesis and the blood-testis barrier [43]. The present study shows that *Smtnl2* is expressed in mouse granulosa cells and the lack of *Nts* expression increased *Smtnl2* expression. This implies that reduced *Smtnl2* expression by NTS could regulate ovarian blood flow, thus facilitating follicle rupture.

In summary, these findings reveal that hCG-induced *Nts* regulates several novel genes that could potentially impact the ovulatory process thereby promoting ovulation and corpus luteum formation.

Supplementary material

Supplementary material is available at *BIOLRE* online.

Authors' contributions

KS: designed study, performed research, analyzed data, and wrote the paper. LAA: performed research, and analyzed data. PG: performed research, and analyzed data. MW: performed research, and analyzed data. PRH: analyzed data and wrote the paper. MJ: designed study, analyzed data, and wrote the paper. JD: analyzed data. DMD: designed study, analyzed data, and wrote the paper. TEC: designed study, performed research, analyzed data, and wrote the paper.

Data availability

The data underlying this article are available in Gene Expression Omnibus (GEO) database. The accession number is GSE210811.

Conflict of interest

The authors have declared that no conflict of interest exists.

References

1. Peng XR, Hsueh AJW, Lapolt PS, Bjersing L, Ny T. Localization of luteinizing hormone receptor messenger ribonucleic acid expression in ovarian cell types during follicle development and ovulation. *Endocrinology* 1991; **129**:3200–3207.

2. al-Alem L, Puttabyatappa M, Shrestha K, Choi Y, Rosewell K, Brännström M, Akin J, Jo M, Duffy DM, Curry TE Jr. Neurotensin: a neuropeptide induced by hCG in the human and rat ovary during the periovulatory period. *Biol Reprod* 2021; **104**:1337–1346.

3. Campbell GE, Bender HR, Parker GA, Curry te Jr, Duffy DM. Neurotensin: a novel mediator of ovulation? *FASEB J* 2021; **35**:e21481.

4. Kalafatakis K, Triantafyllou K. Contribution of neurotensin in the immune and neuroendocrine modulation of normal and abnormal enteric function. *Regul Pept* 2011; **170**:7–17.

5. Li J, Song J, Zaytseva YY, Liu Y, Rychahou P, Jiang K, Starr ME, Kim JT, Harris JW, Yiannikouris FB, Katz WS, Nilsson PM *et al.* An obligatory role for neurotensin in high-fat-diet-induced obesity. *Nature* 2016; **533**:411–415.

6. Osadchii OE. Emerging role of neurotensin in regulation of the cardiovascular system. *Eur J Pharmacol* 2015; **762**:184–192.

7. Wissing ML, Kristensen SG, Andersen CY, Mikkelsen AL, Høst T, Borup R, Grøndahl ML. Identification of new ovulation-related genes in humans by comparing the transcriptome of granulosa cells before and after ovulation triggering in the same controlled ovarian stimulation cycle. *Hum Reprod* 2014; **29**:997–1010.

8. Hiradate Y, Inoue H, Kobayashi N, Shirakata Y, Suzuki Y, Gotoh A, Roh SG, Uchida T, Katoh K, Yoshida M, Sato E, Tanemura K. Neurotensin enhances sperm capacitation and acrosome reaction in mice. *Biol Reprod* 2014; **91**:53.

9. Dias FC, Khan MIR, Sirard MA, Adams GP, Singh J. Differential gene expression of granulosa cells after ovarian superstimulation in beef cattle. *Reproduction* 2013; **146**:181–191.

10. Vincent JP, Mazella J, Kitabgi P. Neurotensin and neurotensin receptors. *Trends Pharmacol Sci* 1999; **20**:302–309.

11. Mazella J. Sortilin/neurotensin receptor-3: a new tool to investigate neurotensin signaling and cellular trafficking? *Cell Signal* 2001; **13**:1–6.

12. Norris EJ, Zhang Q, Jones WD, DeStephanis D, Sutker AP, Livasy CA, Ganapathi RN, Tait DL, Ganapathi MK. Increased expression of neurotensin in high grade serous ovarian carcinoma with evidence of serous tubal intraepithelial carcinoma. *J Pathol* 2019; **248**:352–362.

13. Martin S, Vincent JP, Mazella J. Involvement of the neurotensin receptor-3 in the neurotensin-induced migration of human microglia. *J Neurosci* 2003; **23**:1198–1205.

14. Kleczkowska P, Lipkowski AW. Neurotensin and neurotensin receptors: characteristic, structure-activity relationship and pain modulation–a review. *Eur J Pharmacol* 2013; **716**:54–60.

15. Kim JT, Napier DL, Weiss HL, Lee EY, Townsend CM Jr, Evers BM. Neurotensin receptor 3/sortilin contributes to tumorigenesis of neuroendocrine tumors through augmentation of cell adhesion and migration. *Neoplasia* 2018; **20**:175–181.

16. Akter H, Park M, Kwon OS, Song EJ, Park WS, Kang MJ. Activation of matrix metalloproteinase-9 (MMP-9) by neurotensin promotes cell invasion and migration through ERK pathway in gastric cancer. *Tumour Biol* 2015; **36**:6053–6062.

17. Béraud-Dufour S, Coppola T, Massa F, Mazella J. Neurotensin receptor-2 and -3 are crucial for the anti-apoptotic effect of neurotensin on pancreatic beta-TC3 cells. *Int J Biochem Cell Biol* 2009; **41**:2398–2402.

18. Zhang Y, Zhu S, Yi L, Liu Y, Cui H. Neurotensin receptor1 antagonist SR48692 reduces proliferation by inducing apoptosis

and cell cycle arrest in melanoma cells. *Mol Cell Biochem* 2014; **389**:1–8.

19. Choi Y, Wilson K, Hannon PR, Rosewell KL, Brännström M, Akin JW, Curry TE Jr, Jo M. Coordinated regulation among progesterone, prostaglandins, and EGF-like factors in human ovulatory follicles. *J Clin Endocrinol Metab* 2017; **102**:1971–1982.

20. Jo M, Curry TE Jr. Luteinizing hormone-induced RUNX1 regulates the expression of genes in granulosa cells of rat periovulatory follicles. *Mol Endocrinol* 2006; **20**:2156–2172.

21. Hannon PR, Duffy DM, Rosewell KL, Brännström M, Akin JW, Curry TE Jr. Ovulatory induction of SCG2 in human, nonhuman primate, and rodent granulosa cells stimulates ovarian angiogenesis. *Endocrinology* 2018; **159**:2447–2458.

22. Patro R, Duggal G, Love MI, Irizarry RA, Kingsford C. Salmon provides fast and bias-aware quantification of transcript expression. *Nat Methods* 2017; **14**:417–419.

23. Soneson C, Love MI, Robinson MD. Differential analyses for RNA-seq: transcript-level estimates improve gene-level inferences. *F1000Res* 2015; **4**:1521.

24. McCarthy DJ, Chen Y, Smyth GK. Differential expression analysis of multifactor RNA-Seq experiments with respect to biological variation. *Nucleic Acids Res* 2012; **40**:4288–4297.

25. Chen Y, Lun AT, Smyth GK. From reads to genes to pathways: differential expression analysis of RNA-Seq experiments using Rsubread and the edgeR quasi-likelihood pipeline. *F1000Res* 2016; **5**:1438.

26. RRID:AB_10989085. https://antibodyregistry.org/ search.php?q=AB_10989085.

27. RRID:AB_2192606. https://antibodyregistry.org/search?q=AB_2192606.

28. RRID:AB_2223172. https://antibodyregistry.org/search?q=AB_2223172

29. Ouyang Q, Zhou J, Yang W, Cui H, Xu M, Yi L. Oncogenic role of neurotensin and neurotensin receptors in various cancers. *Clin Exp Pharmacol Physiol* 2017; **44**:841–846.

30. Takahashi K, Ehata S, Miyauchi K, Morishita Y, Miyazawa K, Miyazono K. Neurotensin receptor 1 signaling promotes pancreatic cancer progression. *Mol Oncol* 2021; **15**:151–166.

31. Wu Z, Martinez-Fong D, Trédaniel J, Forgez P. Neurotensin and its high affinity receptor 1 as a potential pharmacological target in cancer therapy. *Front Endocrinol (Lausanne)* 2012; **3**:184.

32. Park KS, Bayles I, Szlachta-McGinn A, Paul J, Boiko J, Santos P, Liu J, Wang Z, Borghesi L, Milcarek C. Transcription elongation factor ELL2 drives Ig secretory-specific mRNA production and the unfolded protein response. *J Immunol* 2014; **193**:4663–4674.

33. Ghobrial A, Flick N, Daly R, Hoffman M, Milcarek C. ELL2 influences transcription elongation, splicing, Ig secretion and growth. *J Mucosal Immunol Res* 2019; **3**. PMID: 31930204.

34. Pascal LE, Masoodi KZ, Liu J, Qiu X, Song Q, Wang Y, Zang Y, Yang T, Wang Y, Rigatti LH, Chandran U, Colli LM *et al.* Conditional deletion of ELL2 induces murine prostate intraepithelial neoplasia. *J Endocrinol* 2017; **235**:123–136.

35. Seo JY, Yaneva R, Cresswell P. Viperin: a multifunctional, interferon-inducible protein that regulates virus replication. *Cell Host Microbe* 2011; **10**:534–539.

36. Seeßle J, Hippchen T, Schnitzler P, Gsenger J, Giese T, Merle U. High rate of HSV-1 reactivation in invasively ventilated COVID-19 patients: immunological findings. *PLoS One* 2021; **16**:e0254129.

37. Russo C, Morello G, Malaguarnera R, Piro S, Furno DL, Malaguarnera L. Candidate genes of SARS-CoV-2 gender susceptibility. *Sci Rep* 2021; **11**:21968.

38. Herrero Y, Pascuali N, Velázquez C, Oubiña G, Hauk V, de Zúñiga I, Peña MG, Martínez G, Lavolpe M, Veiga F, Neuspiller F, Abramovich D *et al.* SARS-CoV-2 infection negatively affects ovarian function in ART patients. *Biochim Biophys Acta Mol Basis Dis* 2022; **1868**:166295.

39. Choi Y, Jeon H, Brännström M, Akin JW, Curry TE Jr, Jo M. Ovulatory upregulation of angiotensin-converting enzyme 2, a receptor for SARS-CoV-2, in dominant follicles of the human ovary. *Fertil Steril* 2021; **116**:1631–1640.

40. Bache KG, Slagsvold T, Cabezas A, Rosendal KR, Raiborg C, Stenmark H. The growth-regulatory protein HCRP1/hVps37A is a subunit of mammalian ESCRT-I and mediates receptor down-regulation. *Mol Biol Cell* 2004; **15**:4337–4346.

41. Wittinger M, Vanhara P, el-Gazzar A, Savarese-Brenner B, Pils D, Anees M, Grunt TW, Sibilia M, Holcmann M, Horvat R, Schemper M, Zeillinger R *et al*. hVps37A Status affects prognosis and cetuximab sensitivity in ovarian cancer. *Clin Cancer Res* 2011; **17**:7816–7827.

42. Gordon EA, Whisenant TC, Zeller M, Kaake RM, Gordon WM, Krotee P, Patel V, Huang L, Baldi P, Bardwell L. Combining docking site and phosphosite predictions to find new substrates: identification of smoothelin-like-2 (SMTNL2) as a c-Jun N-terminal kinase (JNK) substrate. *Cell Signal* 2013; **25**:2518–2529.

43. Wu D, Zhang K, Khan FA, Pandupuspitasari NS, Liang W, Huang C, Sun F. Smtnl2 regulates apoptotic germ cell clearance and lactate metabolism in mouse Sertoli cells. *Mol Cell Endocrinol* 2022; **551**:111664.